

New insights into the nature of the $\Lambda(1380)$ and $\Lambda(1405)$ resonances away from the SU(3) limit

Feng-Kun Guo^{a,b,c}, Yuki Kamiya^d, Maxim Mai^{d,g}, Ulf-G. Meißner^{d,e,f}

^aCAS Key Laboratory of Theoretical Physics, Institute of Theoretical Physics,
Chinese Academy of Sciences, Beijing 100190, China

^bSchool of Physical Sciences, University of Chinese Academy of Sciences, Beijing 100049, China

^cPeng Huanwu Collaborative Center for Research and Education, Beihang University, Beijing 100191, China

^dHelmholtz-Institut für Strahlen- und Kernphysik and Bethe Center for Theoretical Physics,
Universität Bonn, D-53115 Bonn, Germany

^eInstitute for Advanced Simulation, Institut für Kernphysik and Jülich Center for Hadron Physics,
Forschungszentrum Jülich, D-52425 Jülich, Germany

^fTbilisi State University, 0186 Tbilisi, Georgia

^gInstitute for Nuclear Studies and Department of Physics, The George Washington University, Washington, DC 20052, USA

Abstract

Starting from the SU(3) limit, we consider the nature of the dynamically generated resonances $\Lambda(1380)$, $\Lambda(1405)$ and $\Lambda(1680)$ as the pion and kaon masses are tuned to their physical values. We show that the accidental symmetry of the two octets due to the leading order Weinberg-Tomozawa term is broken by the next-to-leading order terms. Most interestingly, we observe an interchange of the two trajectories of the $\Lambda(1380)$ and the $\Lambda(1405)$ away from the SU(3) limit at next-to-leading order. This remarkable phenomenon can be investigated using lattice QCD calculations that start from the SU(3) limit.

1. Introduction

The $\Lambda(1405)$ is a truly exotic hadron state especially after in the framework of unitarized chiral perturbation theory its two-pole structure was revealed and understood [1, 2]. These two states are now called $\Lambda(1380)$ and $\Lambda(1405)$ [3]. For recent reviews, see Refs. [4, 5, 6], and a state-of-the-art calculation with the chiral potential expanded to the next-to-next-to-leading order is given in Ref. [7]. Also, an uncertainty analysis supplemented with an investigation of the correlations between the various poles is presented in Ref. [8].

Lattice studies of the $\Lambda(1405)$ are not very abundant, for earlier works see, e.g., [9, 10]. Of particular interest is the very recent coupled-channel work [11, 12] that also reported two poles consistent with the phenomenological values for $M_\pi \simeq 200$ MeV and $M_K \simeq 487$ MeV. In that study, the lower pole is a virtual state, whereas the higher pole is a resonance.

It is also known that the SU(3) limit, where the u , d , and s quarks have the same mass, can be favorably used in lattice QCD, see, e.g., [13]. To assist such lattice studies and also to gain deeper insight, we study here in detail the development of the poles from the SU(3) flavor limit to the physical masses of the Goldstone bosons.

To be more precise, in the SU(3) limit the interaction of the Nambu-Goldstone (NG) mesons and the octet baryons can be decomposed into group irreducible representations (irreps). By setting up the quark configurations so that they are in the appropriate group representation, we can investigate the interaction in each representation. It was already pointed out that the origin of the two-pole structure of the $\Lambda(1405)$ and $\Lambda(1380)$ resonances is related to the strength of the attractive forces of the decomposed interaction [2]. It was found there that the $\Lambda(1405)$ ($\Lambda(1380)$) pole is connected to the attractive interaction originated in octet (singlet) using a simple extrapolation to the SU(3) limit. Thus, checking these interaction components in the SU(3) limit is helpful in understanding the nature of the $\Lambda(1380)$, $\Lambda(1405)$ and also checking the chiral dynamics. However, such results on the extrapolation from the physical point to the SU(3) limit or some other limit can depend on the detailed scheme of the extrapolation. As found in Ref. [14], where the $a_1(1260)$ is studied varying the number of colors, the trajectory of the two poles in that case may flip depending on

the model details. Thus, to obtain a concrete picture for a given resonance, a detailed scheme for the extrapolation where reasonable parameters are chosen at any hadron mass point in the extrapolation is required.

In this work, we revisit the origin of the $\Lambda(1405)$ and $\Lambda(1380)$ states within chiral dynamics by considering the detailed extrapolation to the SU(3) limit, employing the results from chiral perturbation theory that give the quark-mass dependence of the GB and baryon masses of relevance here. We further consider the $\Lambda(1680)$ that is also generated from the octet. See also Refs. [15, 16] for earlier work along these lines, and Refs. [17, 18] for recent ones. In our work, we go beyond the Weinberg-Tomozawa (WT) term approximation for the meson-baryon interaction potential, and, in particular, we include the next-to-leading order (NLO) operators.

This article is organized as follows. In Sect. 2, we summarize our approach and the scheme for the extrapolation. In Sect. 3, we explain how our model parameters are determined. In Sect. 3 we collect all ingredients of our extrapolation formulas and discuss the evolution of the two poles from the SU(3) limit as the quark masses are tuned to their physical values. Finally, we summarize our study in Sect. 4. In Appendix A, we investigate the poles with quark masses used in the recent lattice calculation [11, 12].

2. Formalism

2.1. Chiral unitary amplitude

In the $\bar{K}N$ system, the WT term, which appears at leading order (LO) in the chiral expansion, gives the dominant contribution to the S -wave interaction. At the same order two one-baryon exchange diagrams contribute, the so-called s - and u -channel Born terms. As common in many studies, we do not consider such LO Born terms here which are negligible in the S -wave projected amplitudes at low energies. The WT interaction term projected to the S -wave and isospin $I = 0$ is given by

$$V_{ij}^{\text{WT}}(\sqrt{s}) = -\frac{C_{ij}^{\text{WT}}}{8F^2} \mathcal{N}_i \mathcal{N}_j (2\sqrt{s} - m_i - m_j) \quad \text{for } i, j \in \{\pi\Sigma, \bar{K}N, \eta\Lambda, K\Xi\}, \quad (1)$$

with the meson decay constant F , the normalization factor $\mathcal{N}_i = \sqrt{m_i + E_i}$, the baryon mass m_i , the baryon energy $E_i = \sqrt{m_i^2 + q_i^2}$, and $q_i = \sqrt{(s - (M_i + m_i)^2)(s - (M_i - m_i)^2)}/(2\sqrt{s})$. The coefficients C_{ij}^{WT} are calculated from the LO chiral Lagrangian and are provided explicitly in, e.g., Refs. [19, 20].

In the SU(3) limit, this interaction term can further be decomposed into irreps. For the meson-baryon system from the octet of the Nambu-Goldstone (NG) bosons and the octet of ground state baryons, the corresponding decomposition of multiplets reads $\{1, 8_s, 8_a, 10, \bar{10}, 27\}$ with the subscripts “s” and “a” referring to the symmetric and antisymmetric representations, respectively, see for more details Refs. [17, 21]. Projecting the above two-particle isoscalar states to the relevant multiplets is accomplished by

$$\begin{pmatrix} |\pi\Sigma\rangle \\ |\bar{K}N\rangle \\ |\eta\Lambda\rangle \\ |K\Xi\rangle \end{pmatrix} = \frac{1}{\sqrt{40}} \begin{pmatrix} \sqrt{15} & -\sqrt{24} & 0 & -1 \\ -\sqrt{10} & -2 & \sqrt{20} & -\sqrt{6} \\ -\sqrt{5} & -\sqrt{8} & 0 & 3\sqrt{3} \\ \sqrt{10} & 2 & 2\sqrt{5} & \sqrt{6} \end{pmatrix} \begin{pmatrix} |1\rangle \\ |8\rangle \\ |8'\rangle \\ |27\rangle \end{pmatrix}, \quad (2)$$

taken from Ref. [22] but correcting for the $i = j = 4$ entry, where $|8\rangle$ and $|8'\rangle$ are mixtures of the symmetric and antisymmetric octets. With this transformation, the WT term diagonalizes as

$$C_{\alpha\beta} = \begin{pmatrix} 6 & 0 & 0 & 0 \\ 0 & 3 & 0 & 0 \\ 0 & 0 & 3 & 0 \\ 0 & 0 & 0 & -2 \end{pmatrix} \quad \text{for } \alpha, \beta \in \{1, 8, 8', 27\}. \quad (3)$$

The crucial observation at this point is that the singlet (1) representation gives the strongest attractive interaction (positive coefficient) while the octet (8) representations also give attraction, noting that the degeneracy of the octets is an accidental symmetry of the WT term, as already discussed in [17]. Noteworthy, the symmetry is broken already

by the LO Born terms, but also by the NLO contact terms discussed below. The (27) representation shows a repulsive (negative coefficient) interaction. The $(10, \bar{10})$ irreps have zero interaction at LO and are not further considered.

We also include the NLO terms, which split into the so-called symmetry breakers ($C^{\text{NLO1}}(b_0, b_D, b_F)$) and dynamical terms ($C^{\text{NLO2}}(d_1, d_2, d_3, d_4)$). We note that the former amplitude vanishes in the chiral limit, but the latter does not. Overall, the NLO potential projected to the S -wave and $I = 0$ is given by

$$V_{ij}^{\text{NLO}}(\sqrt{s}) = \frac{N_i N_j}{F^2} \left(C_{ij}^{\text{NLO1}} - 2C_{ij}^{\text{NLO2}} \left(E_i E_j + \frac{q_i^2 q_j^2}{3N_i N_j} \right) \right) \quad \text{for } i, j \in \{\pi\Sigma, \bar{K}N, \eta\Lambda, K\Xi\}. \quad (4)$$

The coefficients C^{NLO1} and C^{NLO2} are read off from the NLO chiral Lagrangian, and can also be found explicitly in e.g. Ref. [20]. Projected to the relevant multiplets these coefficients read

$$C_{a\beta}^{\text{NLO1}} = \begin{pmatrix} \frac{4}{3}(3b_0 + 7b_D)m_q & 0 & 0 & 0 \\ 0 & \frac{2}{3}(6b_0 + b_D)m_q & -\sqrt{20}b_F m_q & 0 \\ 0 & -\sqrt{20}b_F m_q & 2(2b_0 + 3b_D)m_q & 0 \\ 0 & 0 & 0 & 4(b_0 + b_D)m_q \end{pmatrix}, \quad (5)$$

$$C_{a\beta}^{\text{NLO2}} = \begin{pmatrix} -3d_2 + \frac{9}{2}d_3 + d_4 & 0 & 0 & 0 \\ 0 & \frac{1}{2}(-3d_2 + d_3 + 2d_4) & -\frac{\sqrt{5}}{2}d_1 & 0 \\ 0 & -\frac{\sqrt{5}}{2}d_1 & \frac{1}{2}(9d_2 - d_3 + 2d_4) & 0 \\ 0 & 0 & 0 & \frac{1}{2}(2d_2 + d_3 + 2d_4) \end{pmatrix}. \quad (6)$$

These NLO terms lift the accidental symmetry of the two octets in the $SU(3)$ limit. Note that the Born terms, which we neglect due to its small contribution to the S -wave, also breaks this symmetry. The low-energy constants (LECs) of the symmetry breakers (b_0 , b_D , and b_F) will be determined from the baryon masses as discussed below and the dynamical LECs (d_1 , d_2 , d_3 , and d_4) from a fit to the cross sections $K^- p \rightarrow K^- p, \bar{K}^0 n, \pi^0 \Lambda, \pi^0 \Sigma^0, \pi^\mp \Sigma^\mp$ and usual threshold ratios. For details of these data including data repositories, see the recent review [4].

The attractive interaction between the meson-baryon pair leads to a dynamical generation of the $\Lambda(1405)$ and $\Lambda(1380)$ states. For this a Bethe-Salpeter equation is realized using either WT or WT plus NLO potential in a matrix equation for the unitary scattering amplitude T ,

$$T_{ij} = V_{ij} + \sum_k V_{ik} G_k T_{kj} \quad \text{for } i, j, k \in \{\pi\Sigma, \bar{K}N, \eta\Lambda, K\Xi\}, \quad (7)$$

with V the potential matrix. For the inclusion of off-shell terms and higher partial waves in this type of dynamical equations, see Refs. [23, 24, 25]. Here, the loop function is defined as

$$G_i(\sqrt{s}) = i \int \frac{d^4 q}{(2\pi)^4} \frac{2m_i}{(P - q_i)^2 - m_i^2 + i\epsilon} \frac{1}{q_i^2 - M_i^2 + i\epsilon}, \quad (8)$$

where $M_i(q_i)$ is the meson mass (momentum) of channel i , and the total momentum P is given by $P^\mu = (\sqrt{s}, \mathbf{0})$. Using dimensional regularization, this loop function is given as [1]

$$G_i(\sqrt{s}) = \frac{2m_i}{16\pi^2} \left\{ a_i(\mu) + \ln \frac{m_i^2}{\mu^2} + \frac{M_i^2 - m_i^2 + s}{2s} \ln \frac{M_i^2}{m_i^2} + \frac{\bar{q}_i}{\sqrt{s}} \left[\ln(s - (M_i^2 - m_i^2) + 2\bar{q}_i \sqrt{s}) \right. \right. \\ \left. \left. + \ln(s + (M_i^2 - m_i^2) + 2\bar{q}_i \sqrt{s}) - \ln(-s + (M_i^2 - m_i^2) + 2\bar{q}_i \sqrt{s}) - \ln(-s - (M_i^2 - m_i^2) + 2\bar{q}_i \sqrt{s}) \right] \right\}, \quad (9)$$

where \bar{q}_i is the magnitude of three-momentum in the center-of-mass (c.m.) frame, μ is the scale of dimensional regularization, and $a_i(\mu)$ is the channel-dependent subtraction constant. The values of the subtraction constants in Eq. (9) control the short-distance contributions that are not explicitly considered in the model. It is known that, if the dynamical nature of the system under consideration is well controlled by the chiral interaction, the natural value of $a_i(\mu = 1 \text{ GeV})$ should be around -2 at the physical point, see Ref. [1]. In phenomenological studies, their values

are usually fixed according to a given procedure (see below) or tuned so that the experimental data or lattice results are well reproduced. However, the subtraction constant depends on details of the system, e.g., hadron masses. Thus, these values can gradually change in the extrapolation from the physical point to the SU(3) limit. There are different procedures of fixing the subtraction constants. Here, we follow the scheme proposed in Refs. [26, 27], which requires the loop function to satisfy the relation

$$G(\sqrt{s} = m_B; a(\mu)) = 0 \iff T(\mu) = V(\mu), \quad (10)$$

with $\mu = m_B$ the physical mass of the involved baryon. In this way, given the hadron masses, we can determine a value of the subtraction constant. Note that, in the SU(3) limit, all the baryon masses are equal so that there is effectively only a single subtraction constant.

2.2. Quark mass dependence of the NG bosons

Up to one-loop order, the pion mass dependence of the NG boson masses $\{M_P | P = \pi, K, \eta\}$ are provided through chiral perturbation theory [28] reading

$$\begin{aligned} M_\pi^2 &= M_{0\pi}^2 \left[1 + \mu_\pi - \frac{\mu_\eta}{3} + \frac{16M_{0K}^2}{F_0^2} (2L_6^r - L_4^r) + \frac{8M_{0\pi}^2}{F_0^2} (2L_6^r + 2L_8^r - L_4^r - L_5^r) \right], \\ M_K^2 &= M_{0K}^2 \left[1 + \frac{2\mu_\eta}{3} + \frac{8M_{0\pi}^2}{F_0^2} (2L_6^r - L_4^r) + \frac{8M_{0K}^2}{F_0^2} (4L_6^r + 2L_8^r - 2L_4^r - L_5^r) \right], \\ M_\eta^2 &= M_{0\eta}^2 \left[1 + 2\mu_K - \frac{4}{3}\mu_\eta + \frac{8M_{0\eta}^2}{F_0^2} (2L_8^r - L_5^r) + \frac{8}{F_0^2} (2M_{0K}^2 + M_{0\pi}^2)(2L_6^r - L_4^r) \right] \\ &\quad + M_{0\pi}^2 \left(-\mu_\pi + \frac{2}{3}\mu_K + \frac{1}{3}\mu_\eta \right) + \frac{128}{9F_0^2} (M_{0K}^2 - M_{0\pi}^2)^2 (3L_7^r + L_8^r), \end{aligned} \quad (11)$$

where M_{0P} is the NG boson mass at leading chiral order, and $L_i^{(r)}$ are the renormalized NLO LECs. Furthermore, $\mu_P = M_{0P}^2/(32\pi^2 F_0^2) \log(M_{0P}^2/\mu^2)$ for $P = \pi, K, \eta$. Note that the LEC L_7 does not get renormalized and that in Ref. [28] the LO masses inside the square brackets are substituted by the physical masses. The latter is allowed as the difference from the above expressions is of higher (two-loop) order. The LO masses are related to the constant B_0 and the quark masses $\hat{m} = (m_u + m_d)/2$ and m_s as

$$M_{0\pi}^2 = 2\hat{m}B_0, \quad M_{0K}^2 = (\hat{m} + m_s)B_0, \quad M_{0\eta}^2 = \frac{2}{3}(\hat{m} + 2m_s)B_0, \quad (12)$$

where isospin breaking effects have been neglected. The relations for the decay constants of the NG bosons are given as [28]

$$\begin{aligned} F_\pi &= F_0 \left[1 - 2\mu_\pi - \mu_K + \frac{4M_{0\pi}^2}{F_0^2} (L_4^r + L_5^r) + \frac{8M_{0K}^2}{F_0^2} L_4^r \right], \\ F_K &= F_0 \left[1 - \frac{3\mu_\pi}{4} - \frac{3\mu_K}{2} - \frac{3\mu_\eta}{4} + \frac{4M_{0\pi}^2}{F_0^2} L_4^r + \frac{4M_{0K}^2}{F_0^2} (2L_4^r + L_5^r) \right], \\ F_\eta &= F_0 \left[1 - 3\mu_K + \frac{4L_4^r}{F_0^2} (M_{0\pi}^2 + 2M_{0K}^2) + \frac{4M_{0\eta}^2}{F_0^2} L_5^r \right]. \end{aligned} \quad (13)$$

Approaching the SU(3) limit these quark mass dependencies simplify strongly and can be written compactly as

$$\begin{aligned} M_{\text{SU}(3)} &= M_{0,\text{SU}(3)}^2 \left[1 - \frac{2}{3}\mu_{\text{SU}(3)} \frac{8M_{0,\text{SU}(3)}^2}{F_0^2} (-3L_4^r - L_5^r + 6L_6^r + 2L_8^r) \right], \\ F_{\text{SU}(3)} &= F_0 \left[1 - 3\mu_{\text{SU}(3)} + \frac{4M_{0,\text{SU}(3)}^2}{F_0^2} (3L_4^r + L_5^r) \right], \end{aligned}$$

Table 1: The determined parameters for the extrapolation. For the mesons, the LO masses and the meson decay constant in the chiral limit from the fit are listed. For the baryons, the chiral limit mass m_0 and the symmetry breaking LECs are listed.

$M_{0,\pi}$ [MeV]	$M_{0,K}$ [MeV]	F_0 [MeV]	L_7	m_0 [MeV]	b_0 [GeV ⁻¹]	b_D [GeV ⁻¹]	b_F [GeV ⁻¹]
125.0	443.4	79.3	-4.48×10^{-4}	844.9	-0.43	0.08	-0.27

Table 2: Meson and baryon masses as well as meson decay constants calculated with the fitted LECs. All units are MeV.

m_N	m_Λ	m_Σ	m_Ξ	M_π	M_K	M_η	F_π	F_K	F_η
940.9	1111.5	1191.6	1322.2	137.3	495.6	547.9	92.4	112.7	121.7

where $M_{\text{SU}(3)}$ and $F_{\text{SU}(3)}$ are the meson mass and decay constant in the SU(3) limit, $M_{0,\text{SU}(3)}$ is the LO mass, and F_0 is decay constant in the chiral limit and does not depend on the quark masses. Furthermore, $\mu_{\text{SU}(3)} = M_{0,\text{SU}(3)}^2 / (32\pi^2 F_0^2) \times \log(M_{0,\text{SU}(3)}^2 / \mu^2)$.

In this study, we employ the L_i values obtained in Fit 1 in Ref. [29] where the experimental and lattice meson-meson scattering data are fitted. In Sect 3, we determine the M_{0P} values by fitting to the physical and lattice meson masses.

2.3. Quark mass dependence of octet baryon masses

For the octet baryon masses, the chiral extrapolations are written down up to the fourth order in chiral expansion in Refs. [30, 31]. Within chiral perturbation theory, the baryon mass is written down generally as

$$m_B = m_0 + m_B^{(2)} + m_B^{(3)} + m_B^{(4)} + \dots, \quad (14)$$

where m_0 is the baryon mass in the chiral limit ($\hat{m} = m_s = 0$), and $m_B^{(i)}$'s are the terms of the order of M_p^i . Here, we take into account terms up to $m_B^{(2)}$ to avoid the appearance of large kaon and eta loops and the related convergence problems [30]. In the isospin symmetric case, the LO term of $m_B^{(2)}$ is given as

$$m_B^{(2)} = \gamma_{1,B} B_0 \hat{m} + \gamma_{2,B} B_0 m_s, \quad (15)$$

where the coefficients $\gamma_{i,B}$ are

$$\begin{aligned} \gamma_{1,\Sigma} &= -8(b_0 + b_D), & \gamma_{2,\Sigma} &= -4b_0, & \gamma_{1,N} &= -8b_0 - 4(b_D + b_F), & \gamma_{2,N} &= 4(-b_0 - b_D + b_F), \\ \gamma_{1,\Xi} &= -8b_0 + 4(-b_D + b_F), & \gamma_{2,\Xi} &= -4(b_0 + b_D + b_F), & \gamma_{1,\Lambda} &= -8b_0 - \frac{8}{3}b_D, & \gamma_{2,\Lambda} &= -4b_0 - \frac{16}{3}b_D, \end{aligned} \quad (16)$$

where b_0, b_D and b_F are the aforementioned symmetry-breaking LECs. In the SU(3) limit with $\hat{m} = m_s$, this reduces to

$$m_B^{(2)} = (-12b_0 - 8b_D) B_0 \hat{m}. \quad (17)$$

Given m_0, b_0, b_D and b_F , the baryon masses at any unphysical quark masses can be evaluated. However, with only the physical hadron masses, m_0 and b_0 cannot be fixed independently. This is because these parameters give a common contribution of $(m_0 - 12b_0 B_0 \hat{m})$ to every octet baryon mass. To separate these two LECs, one would have to consider, e.g., the pion-nucleon σ term [30] or baryon masses at unphysical quark masses.

3. Nature of the Λ resonances for varying pion and kaon masses

3.1. Parameters and trajectories

The quark mass dependence provided in the previous section serves as a guideline to define a trajectory from the SU(3) symmetric point to the physical one. In that, we first need to determine the pertinent LECs for the mesons and

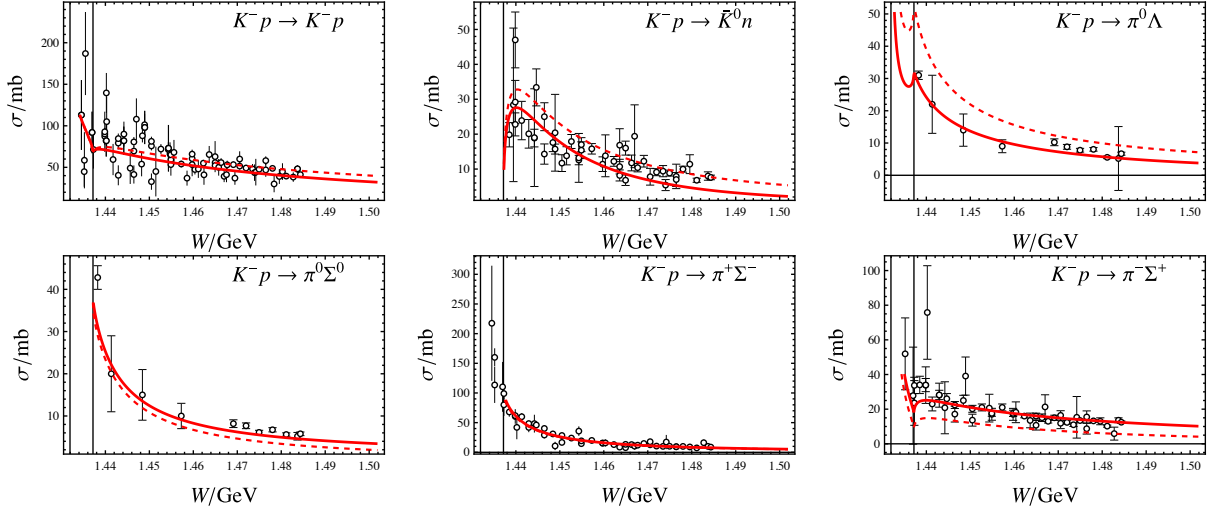


Figure 1: Fit to the experimental data for $K^- p$ scattering. For the source of the data, see the review [4]. Solid (dashed) lines: NLO (WT) fit.

baryons. Following the procedure of Ref. [16], $M_{0,p}$ and F_0 are determined by fitting to the isospin averaged values of the physical meson masses M_π , M_K and M_η , and the pion decay constant F_π . In this procedure, the LEC L_7 is refitted so that these four physical values are well reproduced. The obtained values are summarized in Table 1 which then leads to the well-reproduced meson masses provided in Table 2. In the same time the fitted L_7 is very close to original value of -4.4×10^{-4} [28].

Next, we determine the parameters m_0 , b_D , and b_F for the baryon masses. To this end, we fit the isospin averaged values of the octet baryon masses m_N , m_Λ and m_Σ . Additionally, the baryon masses were obtained in the lattice QCD calculation at unphysical quark masses in, e.g., Ref. [10], and using these values we determine m_0 and b_0 separately. Among the lattice sets in Ref. [10], we employ the heaviest one for which the isospin averaged baryon mass is 1444.2 MeV and the isospin averaged octet meson mass is 659.4 MeV. In this case, the pion mass dependence is such that the LECs m_0 and b_0 can easily be separated. The resulting parameters are also listed in Table 1. The obtained value for m_0 is consistent with the one obtained in the two-flavor expansion in chiral perturbation theory supplemented with the pion-nucleon sigma term from Roy-Steiner equations [32]. The difference to that value can be attributed to the strangeness sigma term. The Ξ baryon mass, which is not fitted in this procedure, is obtained as $m_\Xi = 1322.2$ MeV and is close to the experimental value of 1318.3 MeV.

We fix the subtraction constant in each channel with the scale of dimensional regularization equal to the physical baryon mass in that channel from the condition in Eq. (10),

$$a_{\pi\Sigma} = -0.70, \quad a_{K^0 N} = -1.15, \quad a_{\eta\Lambda} = -1.21, \quad a_{K^0 \Xi} = -1.13. \quad (18)$$

At the SU(3) symmetric point these parameters approach a common value of

$$a_{\text{SU}(3)} = -0.92, \quad (19)$$

through the condition in Eq. (10). Including the NLO part (4) requires additionally the knowledge of further (dynamical and symmetry-breaking) LECs. For the symmetry breakers, we take the values determined through the running of the baryon masses, quoted in Table 1. The dynamical LECs are determined through a fit to experimental data at the physical point, including the usual total cross sections (restricting laboratory momentum of the kaon to $P_{\text{LAB}} = 300$ MeV, see Fig. 1) and the usual threshold values, including kaonic hydrogen data from Ref. [33]. Provided the fact that Born terms are excluded from the potential kernel and the number of free parameters (d_1, d_2, d_3, d_4) is small, we obtained a reasonable fit for

$$d_1 = -0.36, \quad d_2 = 0.09, \quad d_3 = 0.10, \quad d_4 = -0.59. \quad (20)$$

in units of GeV^{-1} . These are values of natural size. For the kaonic hydrogen and threshold ratios we get $\Delta E - i\Gamma/2 = 356 - i464 \text{ eV}$, $\gamma = 2.38$, $R_c = 0.19$, $R_n = 0.65$ compared to the experimental values $\Delta E - i\Gamma/2 = 283 \pm 42 - i542 \pm 110 \text{ eV}$, $\gamma = 2.38 \pm 0.04$, $R_c = 0.19 \pm 0.02$, $R_n = 0.66 \pm 0.01$. While this fit is not perfect, we do not expect any qualitative changes of the results to be discussed.

3.2. Pole positions

For the physical hadron masses listed in Table 2, the pole positions of the $\Lambda(1380)$, $\Lambda(1405)$ and $\Lambda(1680)$ resonances at LO and NLO are found as

$$\begin{aligned} E_{\Lambda(1380)}^{\text{LO}} &= 1403.3 - i80.3 \text{ MeV}, & E_{\Lambda(1380)}^{\text{NLO}} &= 1415.4 - i165.7 \text{ MeV}, \\ E_{\Lambda(1405)}^{\text{LO}} &= 1422.7 - i16.2 \text{ MeV}, & E_{\Lambda(1405)}^{\text{NLO}} &= 1417.9 - i15.7 \text{ MeV}, \\ E_{\Lambda(1680)}^{\text{LO}} &= 1717.4 - i22.9 \text{ MeV}, & E_{\Lambda(1680)}^{\text{NLO}} &= 1725.9 - i13.7 \text{ MeV}. \end{aligned} \quad (21)$$

The first two resonance poles are located between the $\pi\Sigma$ and $\bar{K}N$ thresholds. We note that the heavier pole agree better with the values quoted by the PDG [3]. The width of the broad $\Lambda(1380)$ changes rapidly between the LO and NLO estimations, which is also quite uncertain in the literature values [3], see also the discussion in Ref. [4]. The situation is similar to the lower pole of the scalar charmed meson $D_0^*(2300)$: the width increases sizably from LO [34] to NLO [35]. For the purpose of the present paper, a discussion of the SU(3) trajectories, we consider the determined pole positions as a fair representation of the realistic values. Additionally, using the decay constants and hadron masses from Refs. [11, 12] we have also extracted the poles using our coupled-channel chiral unitary approach, see Appendix A, noting a number of systematic effects that can affect the positions and the nature of the these poles.

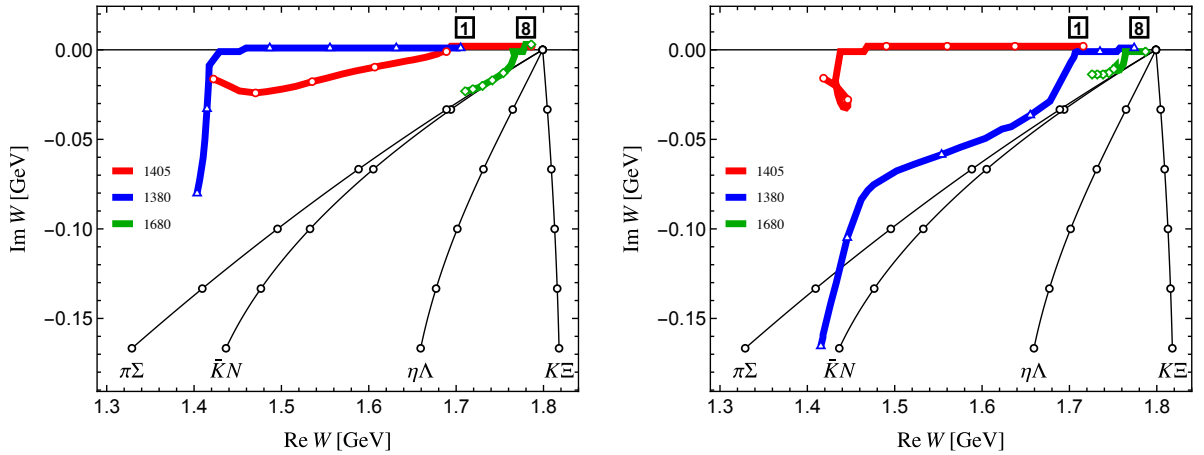


Figure 2: Motion of the poles from the SU(3) limit to the physical values of the particle masses ((0.0, 0.2, ..., 1.0) steps are shown by the empty dots). The blue, red, green lines denote the $\Lambda(1380)$, $\Lambda(1405)$ and $\Lambda(1680)$ in order. Left panel: WT-interaction. Right panel: including the NLO terms. Upper/Lower half-plane correspond to physical/unphysical sheets (small displacement along the real energy axis is added/subtracted for clarity). In both figures, numbers in black boxes denote the multiplet to which the poles belong to in the SU(3) limit. The various meson-baryon thresholds are also shown as the black solid lines.

Next, we consider the SU(3) limit, noting first that there is only one two-body threshold at $E \approx 1799 \text{ MeV}$. This implies that while there are originally 2^4 Riemann sheets, they collapse in the SU(3) limit to only two. Looking for the physically relevant pole content we find in both (LO and NLO) approaches three poles on the real axis. Notably, for the former scenario the previously discussed accidental symmetry of the WT terms prohibits the $8/8'$ mixing and leads to two degenerate octet poles. Specifically, we record three poles on the physical Riemann sheet for the LO WT-interaction: $\{E^1 = 1704 \text{ MeV}, E^8 = 1788 \text{ MeV}, E^{8'} = 1788 \text{ MeV}\}$. Including the NLO terms breaks this accidental symmetry, and we record three separated poles $\{E^1 = 1716 \text{ MeV}, E^8 = 1772 \text{ MeV}, E^{8'} = 1787 \text{ MeV}\}$ where both the

former poles are located on the physical Riemann sheet and the latter one is located on the unphysical sheet. We note that overall the shifts due to the NLO terms are rather small in this limit.

An interesting observation can be made when trying to connect the three poles in the SU(3) limit to those at the physical point. This is depicted in Fig. 2. We observe there that the trajectory of the $\Lambda(1680)$ stays essentially the same in the LO and NLO formalisms up to the fact that the latter does not seem to reach into the physical sheet and the state remains a virtual state. Since the remaining path of the pole is quite small, we argue that this may be due to the details of the model (goodness of the NLO fit, inclusion of Born terms etc.). However, dramatic changes due to the inclusion of the NLO terms occur for the trajectories of the $\Lambda(1380)$ and $\Lambda(1405)$. There, we see that the SU(3) limit results are not that different, but the poles in that limit extend to different poles at the physical point. In other words, the $\Lambda(1380)$ originates in LO/NLO from the singlet/octet state in the SU(3) limit, while $\Lambda(1405)$ originates in LO/NLO from the octet/singlet state in the SU(3) limit. This interchange of trajectories is a surprising new feature not expected from the pioneering study of Ref. [2]. Obviously, one can argue that the fit is not perfect and more details or possibly next-to-next-to-leading order terms need to be included. Additionally, close to the SU(3) limit thresholds are very close to each other, such that identification of individual poles is complicated. Still, indubitably the pole trajectories can change their behavior, which is also demonstrated in Fig. 3. There, as an example we begin with the NLO trajectory of the $\Lambda(1380)$ but scale then the NLO terms with a prefactor $x \in [0, 1]$, i.e., for $x = 0/1$ one obtains back the LO/NLO trajectory. We observe that between $x = 0.33$ and $x = 0.66$ the trajectory indeed changes from that connected to the more bound state to the less bound one in the SU(3) limit. In fact, this interconnection between these trajectories of the $\Lambda(1380)$ and the $\Lambda(1405)$ is quite reasonable from the recent detailed study of the correlations between $\Lambda(1380)$ and $\Lambda(1405)$ in Ref. [8].

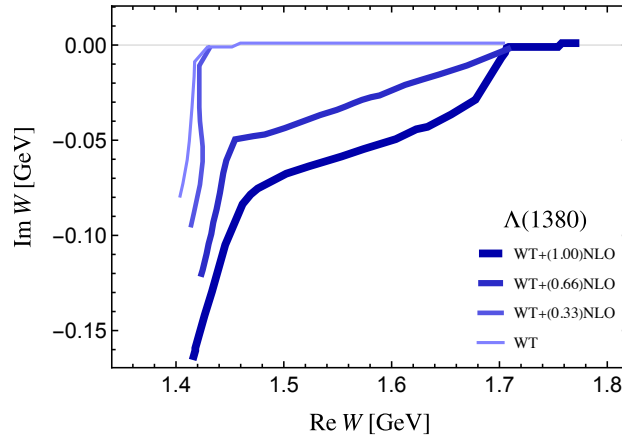


Figure 3: Trajectories of the $\Lambda(1380)$ pole from the SU(3) limit for smoothly varied NLO terms. The numbers in front of “NLO” in the legend denote the prefactor multiplied to the NLO potential.

4. Summary

It has been suggested since long that the $\Lambda(1405)$ has a two-pole structure, thus corresponding to two states $\Lambda(1380)$ and $\Lambda(1405)$, and the lowest negative-parity baryons are dynamically generated from unitarizing the chiral amplitude. In quark model, baryons composed of three quarks can form an SU(3) flavor singlet and two SU(3) octets. In the dynamical generation picture, among all the SU(3) multiplets, also only the singlet and two octets have S -wave attractive interactions from the LO chiral dynamics and lead to dynamically generated states. While the mass differences among states in different multiplets depend on quark model details in the three-quark picture, they follow chiral dynamics in the dynamical generation picture. This essential difference can be checked using lattice calculations by computing baryon spectrum in the SU(3) limit and by varying quark masses from the SU(3) limit to more realistic values, see Refs. [11, 12] for a recent attempt.

In this study, we have discussed the $\Lambda(1380)$, $\Lambda(1405)$ and $\Lambda(1680)$ resonances in the SU(3) limit and the evolution of their poles away from the SU(3) limit within chiral SU(3) dynamics. The poles are generated by unitarizing the

LO chiral amplitude in the WT approximation and also including the NLO terms. We find that the $\Lambda(1405)$ state has always two different poles for any SU(3) limit, one in singlet and the other in octet, and the $\Lambda(1680)$ is degenerate with the heavier pole at LO in that limit. The degeneracy is an artifact of unitarizing only the WT chiral amplitude at LO and is removed by considering higher order contributions (even by considering the Born terms at LO). We have worked out the pole trajectories corresponding to these states when one moves away from the SU(3) limit. Most interestingly, we find that the trajectories of the $\Lambda(1380)$ and the $\Lambda(1405)$ change roles when going from the WT term at LO to the NLO contributions. This phenomenon can be further studied on the lattice when starting with an SU(3) symmetric configuration and then evolving to the physical light and strange quark masses.

Acknowledgements

We thank Tetsuo Hyodo for contributions during the early stage of this work, which started in 2019. We also thank Aleš Cieplý and Peter Bruns for useful discussions on related topics. This work is supported in part by the DFG (Project number 196253076 - TRR 110) and the NSFC (Grant No. 11621131001) through the funds provided to the Sino-German CRC 110 “Symmetries and the Emergence of Structure in QCD”, by the Chinese Academy of Sciences (CAS) through a President’s International Fellowship Initiative (PIFI) (Grant No. 2018DM0034), by the VolkswagenStiftung (Grant No. 93562), by the EU Horizon 2020 research and innovation programme, STRONG-2020 project under grant agreement No. 824093, by the NSFC under Grant Nos. 12125507, 11835015 and 12047503, and by CAS under Grant Nos. YSBR-101 and XDB34030000.

Appendix A. Investigating the Baryon Scattering Collaboration poles

The Baryon Scattering Collaboration [11, 12] has performed a two-channel analysis ($\pi\Sigma\bar{K}N$) in the region of the $\Lambda(1405)$ for unphysical hadron masses and decay constants $M_\pi = 203.7$ MeV, $M_K = 486.4$ MeV, $M_\eta = 551.1$ MeV, $F_\pi = 93.2$ MeV, $F_K = 108.2$ MeV, $m_N = 979.8$ MeV, $m_\Lambda = 1132.8$ MeV, $m_\Sigma = 1193.9$ MeV. For the remaining required parameters we take the usual values $F_\eta = 1.3F_\pi$, $M_\Xi = 1322.2$ MeV. With these values we solve the Bethe-Salpeter equation (7) at leading order (WT-interaction) and including the NLO interactions.

In exploring lattice setups with chiral unitary approaches certain subtleties can arise in, e.g., how the decay constants are used or how the lattice errors on the hadron masses are propagated, see Ref. [36] for an in-depth discussion of such effects. In the current work we have explored two ways to give a sense of the systematic uncertainty. Namely, we use either subtraction constants at the physical point or those from the condition in Eq. (10) for the WT and NLO-interactions, correspondingly. This yields the pole positions on the physical (top half-plane) and unphysical ($\{-++\}$ lower half-plane) Riemann sheet as depicted in Fig. A.4. We note that in certain scenarios the high-mass or the low-mass pole agrees astonishingly well with the analysis of Ref. [11]. Still it is important to note that through a chiral trajectory poles can transition from the unphysical Riemann sheet to the physical, c.f. NLO1 vs. LO1 solutions for the $\Lambda(1380)$ in Fig. A.4. From the findings displayed here it is obvious that one cannot make a definite statement about the nature of the low-mass pole. In the future one should reanalyze the energy levels directly using a coupled-channel chiral approach constrained by experimental data.

References

- [1] J. A. Oller, U.-G. Meißner, Chiral dynamics in the presence of bound states: Kaon nucleon interactions revisited, Phys. Lett. B 500 (2001) 263–272 (2001). [arXiv:hep-ph/0011146](#), [doi:10.1016/S0370-2693\(01\)00078-8](#).
- [2] D. Jido, J. A. Oller, E. Oset, A. Ramos, U.-G. Meißner, Chiral dynamics of the two $\Lambda(1405)$ states, Nucl. Phys. A 725 (2003) 181–200 (2003). [arXiv:nuc1-th/0303062](#), [doi:10.1016/S0375-9474\(03\)01598-7](#).
- [3] R. L. Workman, et al., Review of Particle Physics, PTEP 2022 (2022) 083C01 (2022). [doi:10.1093/ptep/ptac097](#).
- [4] M. Mai, Review of the $\Lambda(1405)$ A curious case of a strangeness resonance, Eur. Phys. J. ST 230 (6) (2021) 1593–1607 (2021). [arXiv:2010.00056](#), [doi:10.1140/epjs/s11734-021-00144-7](#).
- [5] T. Hyodo, M. Niiyama, QCD and the strange baryon spectrum, Prog. Part. Nucl. Phys. 120 (2021) 103868 (2021). [arXiv:2010.07592](#), [doi:10.1016/j.pnpnp.2021.103868](#).
- [6] U.-G. Meißner, Two-pole structures in QCD: Facts, not fantasy!, Symmetry 12 (6) (2020) 981 (2020). [arXiv:2005.06909](#), [doi:10.3390/sym12060981](#).
- [7] J.-X. Lu, L.-S. Geng, M. Döring, M. Mai, Cross-Channel Constraints on Resonant Antikaon-Nucleon Scattering, Phys. Rev. Lett. 130 (7) (2023) 071902 (2023). [arXiv:2209.02471](#), [doi:10.1103/PhysRevLett.130.071902](#).

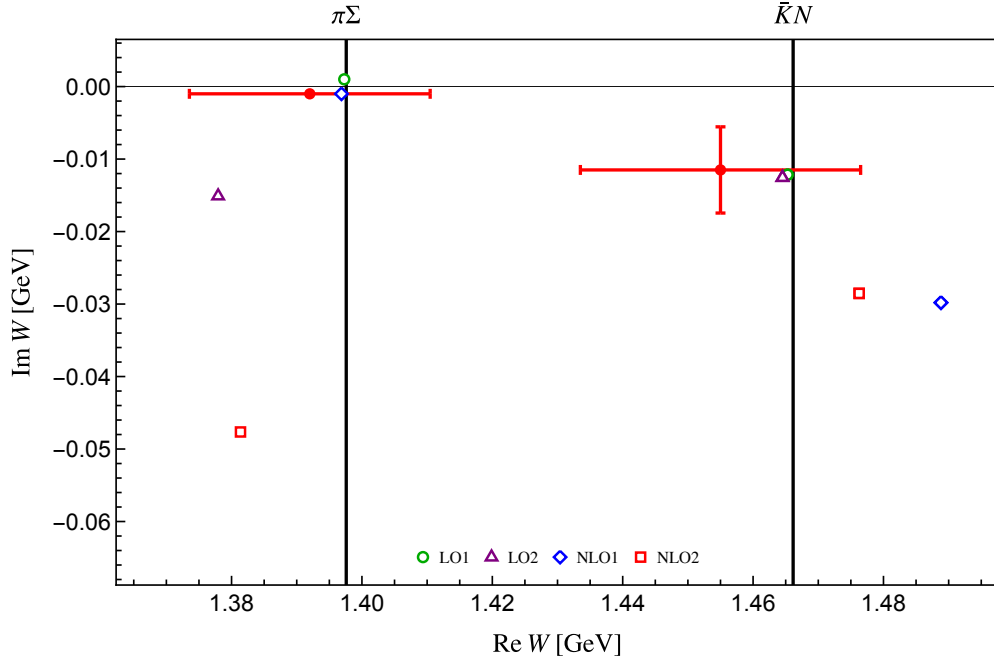


Figure A.4: Predictions for the poles of the $\Lambda(1380)$ and $\Lambda(1405)$ for the lattice setup of Refs. [11, 12]. Green circles/blue diamonds: WT/NLO-interaction with the subtraction constants at the physical point. Purple triangles/red squares: WT/NLO-interaction with the subtraction constants using Eq. (10) with μ set to the corresponding lattice baryon mass. Results of Ref. [11] are depicted by the red dots with statistical and systematic error bars added in quadrature. Upper/lower half plane correspond to the physical/unphysical $\{- + ++\}$ Riemann sheets. Small displacements along the real axis are added for clarity.

- [8] D. Sadasivan, M. Mai, M. Döring, U.-G. Meißner, F. Amorim, J. P. Klucik, J.-X. Lu, L.-S. Geng, New insights into the pole parameters of the $\Lambda(1380)$, the $\Lambda(1405)$ and the $\Sigma(1385)$, Front. Phys. 11 (2023) 1139236 (2023). [arXiv:2212.10415](#), [doi:10.3389/fphy.2023.1139236](#).
- [9] G. P. Engel, C. B. Lang, A. Schäfer, Low-lying Λ baryons from the lattice, Phys. Rev. D 87 (3) (2013) 034502 (2013). [arXiv:1212.2032](#), [doi:10.1103/PhysRevD.87.034502](#).
- [10] J. M. M. Hall, W. Kamleh, D. B. Leinweber, B. J. Menadue, B. J. Owen, A. W. Thomas, R. D. Young, Lattice QCD Evidence that the $\Lambda(1405)$ Resonance is an Antikaon-Nucleon Molecule, Phys. Rev. Lett. 114 (13) (2015) 132002 (2015). [arXiv:1411.3402](#), [doi:10.1103/PhysRevLett.114.132002](#).
- [11] J. Bulava, et al., The two-pole nature of the $\Lambda(1405)$ from lattice QCD (7 2023). [arXiv:2307.10413](#).
- [12] J. Bulava, et al., Lattice QCD study of $\pi\Sigma - \bar{K}N$ scattering and the $\Lambda(1405)$ resonance (7 2023). [arXiv:2307.13471](#).
- [13] W. Bietenholz, et al., Flavour blindness and patterns of flavour symmetry breaking in lattice simulations of up, down and strange quarks, Phys. Rev. D 84 (2011) 054509 (2011). [arXiv:1102.5300](#), [doi:10.1103/PhysRevD.84.054509](#).
- [14] H. Nagahiro, K. Nawa, S. Ozaki, D. Jido, A. Hosaka, Composite and elementary natures of $a_1(1260)$ meson, Phys. Rev. D 83 (2011) 111504 (2011). [arXiv:1101.3623](#), [doi:10.1103/PhysRevD.83.111504](#).
- [15] C. Garcia-Recio, M. F. M. Lutz, J. Nieves, Quark mass dependence of s wave baryon resonances, Phys. Lett. B 582 (2004) 49–54 (2004). [arXiv:nucl-th/0305100](#), [doi:10.1016/j.physletb.2003.11.073](#).
- [16] R. Molina, M. Döring, Pole structure of the $\Lambda(1405)$ in a recent QCD simulation, Phys. Rev. D 94 (5) (2016) 056010, [Addendum: Phys.Rev.D 94, 079901 (2016)] (2016). [arXiv:1512.05831](#), [doi:10.1103/PhysRevD.94.079901](#).
- [17] P. C. Bruns, A. Cieplý, SU(3) flavor symmetry considerations for the K^*N coupled channels system, Nucl. Phys. A 1019 (2022) 122378 (2022). [arXiv:2109.03109](#), [doi:10.1016/j.nuclphysa.2021.122378](#).
- [18] J.-M. Xie, J.-X. Lu, L.-S. Geng, B.-S. Zou, Two-pole structures as a universal phenomenon dictated by coupled-channel chiral dynamics (7 2023). [arXiv:2307.11631](#).
- [19] E. Oset, A. Ramos, Nonperturbative chiral approach to S -wave $\bar{K}N$ interactions, Nucl. Phys. A 635 (1998) 99–120 (1998). [arXiv:nucl-th/9711022](#), [doi:10.1016/S0375-9474\(98\)00170-5](#).
- [20] B. Borasoy, R. Nissler, W. Weise, Chiral dynamics of kaon-nucleon interactions, revisited, Eur. Phys. J. A 25 (2005) 79–96 (2005). [arXiv:hep-ph/0505239](#), [doi:10.1140/epja/i2005-10079-1](#).
- [21] T. Hyodo, D. Jido, A. Hosaka, Study of exotic hadrons in s-wave scatterings induced by chiral interaction in the flavor symmetric limit, Phys. Rev. D 75 (2007) 034002 (2007). [arXiv:hep-ph/0611004](#), [doi:10.1103/PhysRevD.75.034002](#).
- [22] L. Roca, T. Hyodo, D. Jido, On the nature of the $\Lambda(1405)$ and $\Lambda(1670)$ from their N_c behavior in chiral dynamics, Nucl. Phys. A 809 (2008) 65–87 (2008). [arXiv:0804.1210](#), [doi:10.1016/j.nuclphysa.2008.05.014](#).
- [23] P. C. Bruns, M. Mai, U.-G. Meißner, Chiral dynamics of the $S11(1535)$ and $S11(1650)$ resonances revisited, Phys. Lett. B 697 (2011) 254–259

- (2011). [arXiv:1012.2233](#), [doi:10.1016/j.physletb.2011.02.008](#).
- [24] M. Mai, U.-G. Meißner, New insights into antikaon-nucleon scattering and the structure of the Lambda(1405), Nucl. Phys. A 900 (2013) 51–64 (2013). [arXiv:1202.2030](#), [doi:10.1016/j.nuclphysa.2013.01.032](#).
 - [25] D. Sadasivan, M. Mai, M. Döring, S- and p-wave structure of $S = -1$ meson-baryon scattering in the resonance region, Phys. Lett. B 789 (2019) 329–335 (2019). [arXiv:1805.04534](#), [doi:10.1016/j.physletb.2018.12.035](#).
 - [26] M. F. M. Lutz, E. E. Kolomeitsev, Relativistic chiral SU(3) symmetry, large N_c sum rules and meson baryon scattering, Nucl. Phys. A 700 (2002) 193–308 (2002). [arXiv:nucl-th/0105042](#), [doi:10.1016/S0375-9474\(01\)01312-4](#).
 - [27] T. Hyodo, D. Jido, A. Hosaka, Origin of the resonances in the chiral unitary approach, Phys. Rev. C 78 (2008) 025203 (2008). [arXiv:0803.2550](#), [doi:10.1103/PhysRevC.78.025203](#).
 - [28] J. Gasser, H. Leutwyler, Chiral Perturbation Theory: Expansions in the Mass of the Strange Quark, Nucl. Phys. B 250 (1985) 465–516 (1985). [doi:10.1016/0550-3213\(85\)90492-4](#).
 - [29] J. Nebreda, J. R. Peláez, Strange and non-strange quark mass dependence of elastic light resonances from SU(3) Unitarized Chiral Perturbation Theory to one loop, Phys. Rev. D 81 (2010) 054035 (2010). [arXiv:1001.5237](#), [doi:10.1103/PhysRevD.81.054035](#).
 - [30] B. Borasoy, U.-G. Meißner, Chiral Expansion of Baryon Masses and σ -Terms, Annals Phys. 254 (1997) 192–232 (1997). [arXiv:hep-ph/9607432](#), [doi:10.1006/aphy.1996.5630](#).
 - [31] M. Frink, U.-G. Meißner, Chiral extrapolations of baryon masses for unquenched three flavor lattice simulations, JHEP 07 (2004) 028 (2004). [arXiv:hep-lat/0404018](#), [doi:10.1088/1126-6708/2004/07/028](#).
 - [32] M. Hoferichter, J. Ruiz de Elvira, B. Kubis, U.-G. Meißner, Roy–Steiner-equation analysis of pion–nucleon scattering, Phys. Rept. 625 (2016) 1–88 (2016). [arXiv:1510.06039](#), [doi:10.1016/j.physrep.2016.02.002](#).
 - [33] M. Bazzi, et al., A New Measurement of Kaonic Hydrogen X-rays, Phys. Lett. B 704 (2011) 113–117 (2011). [arXiv:1105.3090](#), [doi:10.1016/j.physletb.2011.09.011](#).
 - [34] F.-K. Guo, P.-N. Shen, H.-C. Chiang, R.-G. Ping, B.-S. Zou, Dynamically generated 0^+ heavy mesons in a heavy chiral unitary approach, Phys. Lett. B 641 (2006) 278–285 (2006). [arXiv:hep-ph/0603072](#), [doi:10.1016/j.physletb.2006.08.064](#).
 - [35] M. Albaladejo, P. Fernandez-Soler, F.-K. Guo, J. Nieves, Two-pole structure of the $D_0^*(2400)$, Phys. Lett. B 767 (2017) 465–469 (2017). [arXiv:1610.06727](#), [doi:10.1016/j.physletb.2017.02.036](#).
 - [36] M. Mai, C. Culver, A. Alexandru, M. Döring, F. X. Lee, Cross-channel study of pion scattering from lattice QCD, Phys. Rev. D 100 (11) (2019) 114514 (2019). [arXiv:1908.01847](#), [doi:10.1103/PhysRevD.100.114514](#).